# Renormalization scheme for forest-fire models



1996 J. Phys. A: Math. Gen. 29 2981

(http://iopscience.iop.org/0305-4470/29/12/008)

J. Phys. A: Math. Gen. **29** (1996) 2981–3004. Printed in the UK

# Renormalization scheme for forest-fire models

Vittorio Loreto†, Alessandro Vespignani‡ and Stefano Zapperi§

† Dipartimento di Fisica, Universitá di Roma 'La Sapienza', Piazzale A Moro 2, 00185 Rome, Italy

‡ Instituut-Lorentz, Leiden University, PO Box 9506, 2300RA, Leiden, The Netherlands

§ Center for Polymer Studies and Department of Physics, Boston University, Boston, MA 02215, USA

Received 27 July 1995, in final form 1 February 1996

**Abstract.** We introduce a renormalization scheme for forest-fire models in order to characterize the nature of the critical state and its scale-invariant dynamics. We study one- and two-dimensional models defining a characterization of the phase space that allows us to describe the evolution of the dynamics under a scale transformation. We show the existence of a relevant critical parameter associated with a repulsive fixed point in the phase space. From the renormalization-group point of view these models are therefore critical in the usual sense, because the fixed-point value of the control parameter is crucial in order to get criticality. This general scheme allows us to calculate analytically the critical exponent $\nu$ which describes the approach to the critical point along the repulsive direction and the exponent $\tau$ that characterizes the distribution of forest clusters at the critical point. We obtain $\nu = 1.0$, $\tau = 1.0$ and $\nu = 0.65$, $\tau = 1.16$, respectively, for the one- and two-dimensional cases, in very good agreement with exact and numerical results.

## 1. Introduction

The forest-fire model (FFM) [1, 2] has been introduced as a possible realization of self-organized criticality (SOC) [3–7]. This term refers to the tendency of extended dynamical systems to evolve *spontaneously* in a critical state characterized by spatial and temporal self-similarity. From the point of view of ordinary critical phenomena these systems, in contrast with equilibrium phase transitions, stay close to the critical point for a wide range of the parameter values.

Many examples of systems showing SOC behaviour have been drawn in different fields: geology, biology, economics, etc [8]. In order to illustrate the basic ideas of SOC, Bak and co-workers [3] introduced the so-called sandpile model, a cellular automaton inspired by the dynamics of avalanches in a pile of sand. Dropping sand slowly, grain by grain, on a limited base, one reaches a situation in which the pile is critical, namely it has a critical slope. This means that a further addition of sand will produce slidings of sand (avalanches) that can be small or cover the entire size of the system. In this case the critical state is characterized by scale-invariant distributions for the size and the lifetime of the avalanches. This state represents an attractor for the dynamics and it is reached without the fine tuning of any critical parameter. Other examples of SOC can be found in fractal growth phenomena, such as diffusion-limited aggregation (DLA) [4] and the dielectric breakdown model (DBM) [5] or models like invasion percolation (IP) [7]. These models evolve spontaneously into a statistically stationary state with a self-similar structure.

0305-4470/96/122981+24$19.50  

The forest-fire model was initially introduced by Bak *et al* [1] as a toy model for turbulence. The model is defined on a lattice in which each site can be occupied by a green tree, a burning tree or by ashes. The dynamics contains the tree growth probability $p$ and the fire spreading to nearest neighbours. It was argued that this model shows self-organized criticality in the limit $p \to 0$, namely that the system evolves into a critical stationary state independently of the initial conditions. Large-scale simulations [9, 10] show that the model becomes more and more deterministic and develops spiral-shaped fire fronts. This model is critical but with some trivial critical exponents.

For this reason, the original model was modified by Drossel and Schwabl [2] by introducing an ignition parameter $f$, the lighting parameter. This parameter is the probability that, during one time step, a tree without burning nearest neighbours becomes a burning tree. In this case the system was supposed to exhibit self-organized criticality in the limit of a double time scale separation. This means that the time scale over which a cluster is burned is much smaller than the growth scale of the trees which, in turn, is much smaller than the time scale over which a lightning event occurs. This time scale separation is expressed by the double limit

$$f/p \to 0 \qquad p \to 0\,. \tag{1}$$

Usually the limit $f/p \to 0$ is attributed to the existence of a slow driving of the system, or, in other words, a time scale separation, also present in the definition of sandpile models. In the FFM the parameter $f/p$ directly affects the upper cut-off [11, 12] and seems to play, in the language of ordinary critical phenomena, the role of a relevant parameter. In contrast to sandpile models, it is not possible to consider the the FFM exactly at the critical point, i.e. in a subspace without relevant critical parameters.

To address the study of critical growth phenomena, the fixed-scale transformation approach to fractal growth [13] has been developed and recently we have introduced a renormalization-group (RG) scheme of novel type to study sandpile models [14, 15]. This new method, which has been called a dynamically driven renormalization group (DDRG) [16], is able to describe the self-organized critical state of sandpile models by defining a characterization of the phase space in which it is possible to study the renormalization of the dynamics under a change of scale. In addition the stationary condition characterizes the driving of the system to its steady state. The presence of an attractive fixed point, in a suitable phase space, clarifies the self-organized nature of these systems, at least from the renormalization-group point of view. Finally, it is possible to estimate the critical exponents analytically [14, 15]. It is worth stressing that the DDRG, although inspired by the study of self-organized critical systems, represents a general method to approach non-equilibrium critical systems with a stationary state and it allows us to study equilibrium models at the critical point as well.

In this paper we follow the same ideas of [14, 17] in order to study the one- and two-dimensional FFM including the ignition parameter $f$. The first step of the method is the identification of a suitable phase space to characterize the stationary and dynamical properties of the system. In this phase space we obtain the RG equations which link the dynamical parameters at a generic scale $2b$ with those at scale $b$. We then couple these equations to a stationarity condition which provides the weight of the geometrical configuration in the stationary state. This condition allows us to obtain the renormalized stationary parameters which drive the system in the asymptotic steady state. Studying the flow in the phase space of the RG equations, we find the existence of a repulsive fixed point associated with a relevant critical parameter. This allows us to clarify the role of the critical parameters $\theta$ and $p$, and the nature of the critical state. We evaluate the critical exponents for

the one- and two-dimensional cases. We use different renormalization schemes of increasing complexity, showing the convergence and stability of the method. The results are in good agreement with exact and numerical results.

The outline of the paper is the following. In section 2 we recall the definition of the model and describe the scaling laws characterizing the system; section 3 describes the choice of a suitable set of parameters to characterize the stationary and dynamical properties of the system. Section 4 is devoted to the analysis of the RG transformations in the one-dimensional case. We study the flow of the parameters under a scale transformation and compute the critical exponents analytically. In section 5 we apply the same procedure of section 4 to the two-dimensional case. We implement the procedure for the $2 \times 2$ and the $3 \times 3$ cell schemes and report the calculation of the critical exponents for these cases. The use of more refined calculation schemes allows us to improve the precision of the results. In section 6 alternative schemes of calculation are discussed in order to show that our renormalization scheme is consistent and gives reliable and stable results with respect to the choice of different coarse-graining prescriptions: different spanning condition, majority rules, lattice topologies, etc. Section 7 is devoted to the discussion of the fixed-scale transformation approach for the estimate of the fractal dimension of the fire clusters. Finally, in section 8 we summarize the results and draw the conclusions. Two appendices complete the paper: in appendix A we report the weights of the configurations used in the renormalization procedure in the two-dimensional case in the $2 \times 2$ cell scheme. Appendix B reports the details of the $3 \times 3$ renormalization calculation.

## 2. Forest-fire models

In this section we recall the definition of the model we are going to analyse. The model we consider is a cellular automaton defined on a $d$-dimensional lattice where each site can be found in one of the following configurations: (i) empty site without trees, (ii) green tree and (iii) burning tree.

Starting with arbitrary initial conditions, at each time step the system is updated according to the following dynamical rules:

(i) a burning tree becomes an empty site;

(ii) a green tree becomes a burning tree if at least one of its neighbours is burning;

(iii) a tree can grow with probability $p$ in an empty site;

(iv) a tree without burning nearest neighbours becomes a burning tree with probability $f$.

After a short transient the system approaches a steady state whose properties depend upon the values of the parameters $p$ and $f$. It is useful to define the parameter $\theta = f/p$ whose importance will be discussed later. For this model a critical behaviour, in the sense of anomalous scaling laws, is observed in the double limit $\theta \to 0$ and $p \to 0$. These two limits describe a double time scale separation: trees grow fast compared to the occurrence of lightning in the system and forest clusters burn down much faster than trees grow. In order to describe the critical state of this system a set of critical exponents, whose denomination is directly mutuated from that of sandpile models, can be defined. The critical state is characterized by a power-law distribution

$$P(s) \sim s^{-\tau} \tag{2}$$

of the forest clusters (avalanches in the SOC terminology) of $s$ sites. Other important scaling relations are the following:

$$s \sim R^D \tag{3}$$

$$R \sim \theta^{-\nu} \tag{4}$$

where $R$ is the mean cluster radius. These relations define the fractal dimension $D$ of forest clusters, and the correlation length exponent $\nu$, respectively. Since this critical state is reached independently of the initial conditions and for a wide range of parameter values, it is called the self-organized critical state [2]. This statement is ambiguous, since the requirement of a time scale separation seems to be crucial in order to get criticality and the parameter $\theta$ seems an effective relevant parameter. In this respect the parameter $\theta$ would play the same role as the reduced temperature in thermal phase transitions, in that it allows criticality just for its critical value $\theta = 0$. It is worthwhile stressing how the definition of self-organized criticality is very controversial. If, from the point of view of the RG approach, one could think that SOC is related to the absence of relevant critical parameters, it is also true that one could conceive a situation in which, enlarging the phase space of the sandpile, some relevant parameters appear, e.g. the driving parameter. From this point of view the only difference between sandpile models and forest-fire models would be that forest-fire models cannot be studied in a subspace with no relevant parameters without destroying the model itself. This reasoning can then be rephrased, saying that the peculiarity of the SOC system consists in the fact that the control parameter is always related to the ratio between two time scales with a critical value fixed at zero. In this situation the existence of a time scale separation makes the system always very close to the critical point. The self-organization would then be related to the widespread existence of systems with very different time scales.

In the past few years a lot of work has been done in order to describe the critical state of forest-fire models and to calculate the critical exponents. Numerical simulations [11, 12, 18] showed that in the time scale separation regime the model seems to possess a critical behaviour with the avalanche critical exponent $\tau$ given by $\tau \simeq 1$ in $d = 1$ and $\tau \simeq 1.15$ in $d = 2$. For the exponent $\nu$, describing the divergency of the average cluster radius as $\theta \to 0$, it has been found that $\nu \simeq 1$ in $d = 1$ and $\nu \simeq 0.58$ in $d = 2$. The one-dimensional result has been recovered exactly in [19]. Simulations were also performed in higher dimensions [18, 20]. In the limit $d \to 6$ the exponents approach those of mean-field percolation.

In what follows we will show a renormalization scheme of novel type [17], already applied to sandpile models [14, 15], which allows us to clarify the role of the critical parameters $\theta$ and $p$ and the nature of the critical state. In addition we are able to calculate analytically the critical exponents characterizing the model in $d = 1$ and $d = 2$.

## 3. The renormalization scheme

The renormalization approach we present here is an example of the application of a general method which has been introduced recently, the so-called dynamically driven renormalization group [16]. This method, mainly developed for systems with a non-equilibrium critical stationary state, is based on a real-space renormalization scheme combined with the driving condition which, acting as a feedback on the renormalization equations, characterizes the dynamical evolution to the stationary state. As already pointed out, this method has been applied successfully to the case of sandpile models and also equilibrium models, e.g. the Ising model, at the critical point can be studied in this framework. This general scheme allows for the analytical calculation of scaling dimensions and critical exponents.

In order to develop a renormalization scheme for forest-fire models we have first to

define a suitable phase space in which the RG equations can be obtained. Let $\rho_0$, $\rho_1$ and $\rho_2$ be, respectively, the mean densities of empty sites, green trees and burning trees in the stationary state with the condition $\rho_0 + \rho_1 + \rho_2 = 1$. Thus, $\rho_0$, $\rho_1$ and $\rho_2$ also represent the probabilities that a site is found in one of the three possible states. These probabilities describe in full generality the stationary properties of the model for generic dimensions $d$. For the dynamical properties we will consider a phase space defined by the parameters $p$ and $\theta = f/p$.

We can now extend the characterization of the stationary properties at a generic scale $b$, by considering *coarse-grained variables*. Independently of the dimension $d$ we can define a density vector at the generic scale $b$ as

$$\boldsymbol{\rho}(b) \equiv (\rho_0(b), \rho_1(b), \rho_2(b)) \,. \tag{5}$$

Independently of the minimal scale, a coarse-grained cell of size $b$ is *green* if it is spanned from left to right by a connected path of green sites at scale $b/2$. A cell is *empty* if it is not spanned by a connected path of green sites at the lower scale. Finally, a cell is *burning* if it contains at least one burning tree at the lower scale. In this latter case the spanning condition is not necessary because the fire spreads automatically to nearest-neighbour sites.

In order to describe the dynamical properties at a generic scale $b$ we define the parameters $p(b)$ and $\theta(b)$. The first one represents the growth probability for a green tree at the scale $b$. The second one is given by the ratio between $f(b)$, the probability that a green tree of size $b$ becomes a burning cell because of the arrival of a lightning event, and $p(b)$. We shall define our RG procedure in the phase space $(p(b), \theta(b), \boldsymbol{\rho}(b))$. The parameter $\theta(b)$ is related to the time needed to burn an entire forest cluster at scale $b$. In particular, if we denote by $T(\xi)$ the time needed to burn an entire cluster of characteristic size $\xi$, one has that

$$T(\xi) \sim (f/p)^{-\nu'} \sim \theta^{-\nu'} \tag{6}$$

with $\nu' = \nu z$ [20].

In the actual implementation of the RG scheme we implicitly consider the double time scale separation expressed by $f \ll p \ll 1$. In fact, we will renormalize the tree growth parameter $p$ and the lightning parameter $f$ in separate ways, assuming that they do not affect each other since they act on very different time scales. In addition, one usually considers the model in a further limit in which the time needed to burn an entire cluster of dimension $\xi$ is much smaller than the average time between two tree growths:

$$T(\xi) \ll 1/p \,. \tag{7}$$

This condition corresponds to the requirement that the burning process is instantaneous with respect to the processes of growth and lightning, and it is usually used in the simulations. The advantage of this limit is that one can consider each fire as an isolated event: fires triggered by different lightning events do not overlap, so that clusters destroyed by fire are a well defined object.

In this paper we use the condition (7) in the implementation of the RG procedure. This implies that the fire spreading is instantaneous with respect to the tree growth and the lightning time scales. In this way we can consider the renormalization of $f$ and $p$ completely decoupled from the burning process. This procedure seems to be perfectly adequate for the study of the critical behaviour of the parameter $\theta$, which, being given by the ratio between $f$ and $p$, is not affected by the absolute time scales associated with each of the two parameters.

The condition (7) makes our RG approach suitable for describing what happens in the region of the phase space $(p, \theta)$ described by $p \ll \theta^{\nu'}$. On the other hand, the condition (7) is not really necessary to implement the RG procedure. From [16] we know the most general procedure for the one-dimensional case which, neglecting (7), allows us to study the critical behaviour in all phase space consistent with the conditions $f \ll p \ll 1$.

We discuss separately, for the one- and the two-dimensional case, the explicit form of the RG equations and the coupling between the dynamical and stationary properties at different scales.

## 4. Renormalization equations in one dimension

In this section we define the renormalization transformation for the one-dimensional case. We use a cell-to-site transformation on the lattice in which each cell at the scale $(k+1)$ is composed of two cells at the scale $(k)$. In figure 1 we show the possible configurations corresponding to empty or green cells at scale $(k+1)$. In one dimension a green cell at scale $(k+1)$ is given by two green trees at scale $(k)$.

There are three configurations of sites at scale $(k)$ which give an empty cell at scale $(k+1)$ (figure 1) denoted by $\alpha$. Each configuration has a relative statistical weight $W_\alpha$ given by the probability to have the corresponding number of green and empty subcells:

$$W_1 = W_2 = \frac{\rho_1^{(k)}}{\rho_0^{(k)} + 2\rho_1^{(k)}}$$
$$W_3 = \frac{\rho_0^{(k)}}{\rho_0^{(k)} + 2\rho_1^{(k)}} \,. \tag{8}$$

In order to define a renormalization transformation we start with an empty or green cell configuration at scale $(k+1)$ and we study how it evolves using the dynamical rules of the model. Here we consider a transformation defined by the following rules:

(i) every series of tree growth processes at scale $(k)$ that spans an empty cell at scale $(k+1)$ is renormalized in the growth probability $p$ at scale $(k+1)$;

(ii) every lightning process at scale $(k)$ that affects a green cell at scale $(k+1)$ contributes to the renormalization of the lightning probability $f$.

The spanning rule implies that only tree growth processes extending over the size of the new length scale contribute to the renormalized dynamics. Moreover, it ensures the connectivity properties of the green sites in the renormalization procedure. Figure 2 illustrates the contributions to the renormalization of the growth probability by the empty configuration denoted by $\alpha$. By averaging over all the configurations with their

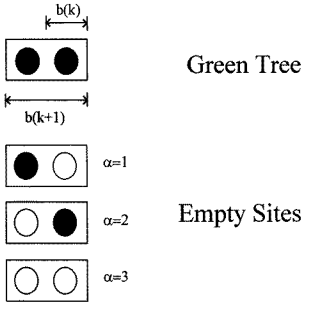


**Figure 1.** The possible configurations of sites at the scale $b^{(k)}$ corresponding to empty or green cells at the scale $b^{(k+1)}$ in $d = 1$.

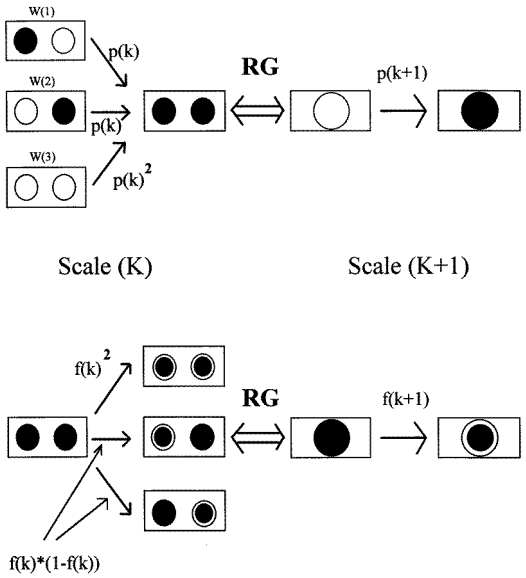


**Figure 2.** Scheme of renormalization of the growth parameter $p$ (up) and of the lightning parameter $f$ (down) in $d = 1$.

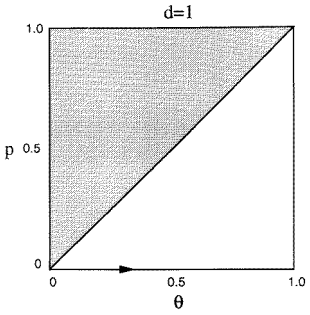


**Figure 3.** Phase space for the RG approach to the one-dimensional forest-fire model. The shadowed region is not described by our RG approach.

corresponding weights we obtain the renormalization equation for $p$:

$$p^{(k+1)} = W_1 p^{(k)} + W_2 p^{(k)} + W_3 (p^{(k)})^2 . \tag{9}$$

In the same way we can write the renormalization equation for $f$ (figure 2):

$$f^{(k+1)} = (f^{(k)})^2 + 2f^{(k)}(1 - f^{(k)}) . \tag{10}$$

The renormalization equations written for $p$ and $\theta$ are therefore given by

$$\begin{aligned} p^{(k+1)} &= (W_1 + W_2) p^{(k)} + W_3 (p^{(k)})^2 \\ \theta^{(k+1)} &= f^{(k+1)}/p^{(k+1)} = \theta^{(k)} \left( \frac{2 - \theta^{(k)} p^{(k)}}{2W_1 + W_3 p^{(k)}} \right) . \end{aligned} \tag{11}$$

These renormalization equations are not yet closed because the statistical weights $W_\alpha$ are a function of the density vector $\boldsymbol{\rho}^{(k)}$. In fact, in order to describe the *stationary critical state* it is necessary to couple the dynamics to a stationarity condition that gives the renormalization equations for the density vector. This scheme is similar to that used in [14].

The stationarity condition can be obtained starting from the master equations for the density vector in the mean-field regime by imposing the asymptotic stationary condition ($t \to \infty$) [18]:

$$\begin{aligned} \rho_0^{(k)} &= (1-\rho_1^{(k)})a^{(k)}/p^{(k)} \\ \rho_1^{(k)} &= \frac{a^{(k)}}{\theta^{(k)}p^{(k)} + 4a^{(k)} - a^{(k)}\rho_1^{(k)}(2d-1)} \\ \rho_2^{(k)} &= (1-\rho_1^{(k)})a^{(k)} \end{aligned} \tag{12}$$

where we defined $a^{(k)} = p^{(k)}/(1+p^{(k)})$, with the normalization condition $\rho_0^{(k)} + \rho_1^{(k)} + \rho_2^{(k)} = 1$.

The stationarity condition, summarized in (12), provides the renormalized density vector at each scale $(k+1)$, and couples the dynamical properties to the stationary ones. It is worth remarking that we do not determine the RG equations for $\boldsymbol{\rho}$ from the coarse-graining prescription. In fact, the stationary properties have to be evaluated considering the average over many dynamical processes. Thus the densities $\boldsymbol{\rho}$ are determined from the renormalized dynamical description of the system, namely (12) with renormalized parameters.

Also note that the RG equations are written with the assumption of a double time scale separation: fire spreading and tree growth are not interacting. This is expressed by the consistency relation $p \ll 1/T(\xi)$. Our RG approach is then suitable to describe what happens in the region of phase space $(p, \theta)$ defined by the condition $p < \theta^{\nu'}$.

Given this scheme, we can thus find the fixed points of the renormalization transformation by studying the flow diagram in phase space of the parameters $(\boldsymbol{\rho}, p, \theta)$. The RG equations (11) and (12) show, for $d = 1$, the fixed point,

$$p^* = 0 \qquad \theta^* = 0 \qquad \boldsymbol{\rho}^* = (0, 1, 0)\,. \tag{13}$$

A complete characterization of the fixed point is obtained by the RG equations linearized around $p^*, \theta^*$ and $\boldsymbol{\rho}^*$ which read as

$$\begin{pmatrix} p' \\ \theta' \end{pmatrix} = \begin{pmatrix} \dfrac{2\rho_1^*}{1+\rho_1^*} & 0 \\ 0 & \dfrac{1+\rho_1^*}{\rho_1^*} \end{pmatrix} \begin{pmatrix} p \\ \theta \end{pmatrix}. \tag{14}$$

The eigenvalues of the previous equation are given by $\lambda_1 = 1.0$ and $\lambda_2 = 2.0$. There is just one relevant scaling field that corresponds to the eigenvalue strictly greater than 1, $\lambda_2 = \mathrm{d}\theta^{(k+1)}/\mathrm{d}\theta^{(k)}$. Therefore we have that the fixed point is repulsive in the $\theta$ direction, which of course defines the relevant control parameter. Since the fixed point is repulsive in the $\theta$ direction, we can determine the exponent of the clusters' characteristic length by the largest eigenvalue $\lambda_2$, and we find

$$\nu = \frac{\log 2}{\log \lambda_2} = 1.0\,. \tag{15}$$

This exponent describes the divergence of the correlation length by $R \sim \theta^{-\nu}$ and it recovers the exact result [19]. In this perspective the parameter $\theta = f/p$ plays the role of the relevant critical parameter as the reduced temperature in the thermal phase transitions. For each value of $\theta$, small but finite, the system shows an upper characteristic length in the cluster distribution. Only for $\theta = 0$ is the system critical and shows an infinite correlation length.

As long as the system is not exactly at the fixed point we have that the forest cluster distribution is defined as follows:

$$P(s) = s^{-\tau} f\left(\frac{s}{s_c}\right) \tag{16}$$

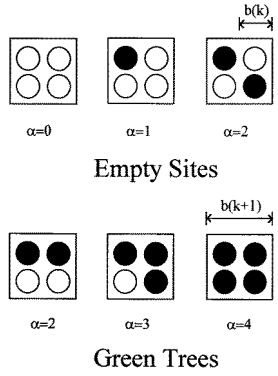


**Figure 4.** The possible configurations of sites at the scale $b^{(k)}$ corresponding to empty or green cells at the scale $b^{(k+1)}$ in $d = 2$ and for the $2 \times 2$ cell scheme.

where $s_c \to \infty$ at the critical point. The function $f(x)$ tends to a constant for $x \ll 1$ and decreases exponentially for $x \gg 1$. For $d = 1$ the avalanche distribution coincides with the distribution for clusters of linear size $r$ and we can easily calculate the exponent $\tau$. In fact, we can use the scaling relation $\nu = 1/(2-\tau)$ [20] which gives the result $\tau = 1$, neglecting logarithmic corrections for $d = 1$. It is worth noting that for $d = 2$ we can no longer use this simple scheme, but we have to calculate $\tau$ using the approach shown in [14].

The calculation of the exponent $z$ is also particularly simple in the one-dimensional case. The dynamical exponent can be defined through the scaling relation linking time and the linear extension of a fire spreading as $T \sim r^z$. Using the discretized length of our scheme, the time scale of a burning process at scale $b^{(k+1)}$ and one at scale $b^{(k)}$ are related in the asymptotic limit ($k \to \infty$) by the relation

$$\frac{T_{k+1}}{T_k} = \langle t \rangle = 2^z \,. \tag{17}$$

The time scaling factor $\langle t \rangle$ is the average number of burning processes at scale $b^{(k)}$ needed to have a fire of length scale $b^{(k+1)}$. The only possible burning process on the scale $b^{(k+1)}$ results from the fire spreading in a green cell at the same scale. Therefore, the number of burning sub-processes needed is $\langle t \rangle = 2$ and from (17) we obtain the result $z = 1$. Consequently, we can also obtain the exponent $\nu'$ which describes the range of validity of our approach and characterizes the double scale separation present in these systems. By substituting the value of $\nu$ and $z$ in the expression $\nu' = \nu z$ we have $\nu' = 1.0$. This implies that our method is able to characterize, in the proximity of the fixed point, the critical behaviour of the model in the lower half of the first quadrant of the (p–$\theta$) plane (see figure 4).

It is interesting to note that our method recovers, in the one-dimensional case, the exact results of the rigorous treatment of [19]. This is due to the relative simplicity of the one-dimensional case, where few approximations are involved in the calculation. For instance, the spanning condition is unique. This is not the case in $d = 2$, where the calculation is much more complicated, and more refined schemes of renormalization are needed.

## 5. Renormalization equations in two dimensions

Here we apply our RG scheme to the forest-fire model in two dimensions, following the same lines as previous sections. The formalism is heavier but only a few differences will emerge with respect to the one-dimensional case.

We consider a phase space described by the parameters $p^{(k)}$, $\theta^{(k)} = f^{(k)}/p^{(k)}$ and $\boldsymbol{\rho}^{(k)}$ at a generic scale $(k)$ with $b^{(k)} = b_0 2^k$. In this case the transformation cell-to-site is such that, on the lattice, each cell at scale $b^{(k+1)}$ is composed by four subcells at scale $b^{(k)}$.

A cell at scale $(k+1)$ is considered *green* if a spanning condition in one direction, say the horizontal direction, is satisfied; a cell is thus green if a fire can span it entirely. On the other hand if the spanning condition is not satisfied the cell is *empty*. Finally, a cell that contains at least a burning subcell is considered *burning*. Figure 4 shows the different configurations at scale $(k)$ which give rise to empty or green sites at scale $(k+1)$. The relative weight of each configuration is given by the probability of having the corresponding number of green and empty subcells

$$W_\alpha(\boldsymbol{\rho}) = \Omega_\alpha \rho_1^\alpha \rho_0^{4-\alpha} \tag{18}$$

where $\alpha$ is the number of green subcells and $\Omega_\alpha$ is a normalization factor depending on $\alpha$. In practice we are approximating the non-equilibrium steady-state statistical weight of the cells with the stationary average density of each configuration. Here we consider the site configurations in the stationary state to be uncorrelated. In some sense this corresponds to a sort of zero cumulant approximation for the stationary statistical distribution. On the other hand, correlations among sites are mainly developed during the dynamical evolution, and consequently, in our scheme correlations are considered in the renormalization equations for the dynamics. For the sake of clarity, in the following we define $W_\alpha^{\mathrm{e}}$ and $W_\alpha^{\mathrm{g}}$ as the relative weights of subcell configurations which give, at scale $(k+1)$ empty or green cells, respectively. The explicit expression of the weights $W_\alpha^{\mathrm{e}}$ and $W_\alpha^{\mathrm{g}}$ is given in appendix A.

The rules to define the renormalization transformation are the same as given in section 4 for the one-dimensional case. Let us start by considering the simplest RG scheme; i.e. $2 \times 2$ cells with a left–right spanning condition.

In figure 5 we show the contributions to the renormalization of $p$ for empty sites at scale $(k+1)$. For $\alpha = 2$, starting with an empty cell at scale $(k+1)$, after an updating step the cell will become green if at least one of the two empty subcells has become green. This occurs with probability $(p^{(k)})^2$ and $2p^{(k)}(1-p^{(k)})$, depending on, respectively, whether both or only one subcell become green.

By summing these probabilities one obtains, for the configuration $\alpha = 2$,

$$p_{\alpha=2}^{(k+1)} = p^{(k)}(2 - p^{(k)})\,. \tag{19}$$

In a similar way we can also write a renormalization equation for each configuration $\alpha$,

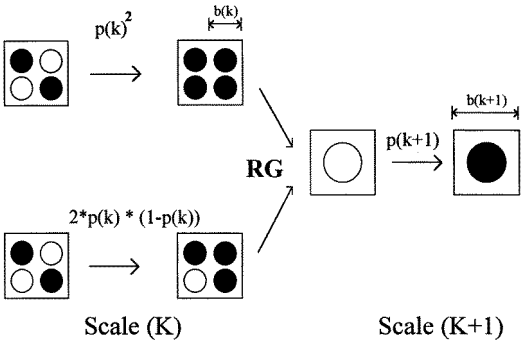


**Figure 5.** Examples of renormalization of the growth parameter $p$ in $d = 2$. The two possible contributions of the configuration $\alpha = 2$ (empty site at the scale $(k+1)$).

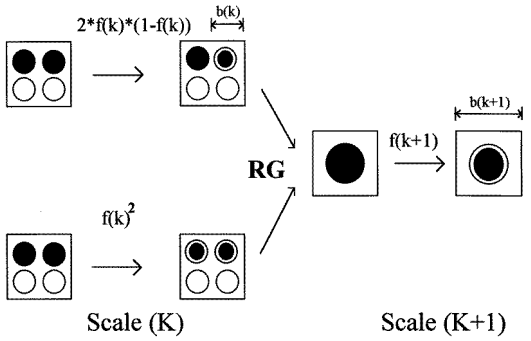


**Figure 6.** Examples of renormalization of the lightning parameter $f$ in $d = 2$. The two possible contributions of the configuration $\alpha = 2$ (green tree at the scale $(k + 1)$).

and, finally averaging over all the configurations with their corresponding weights we obtain

$$p^{(k+1)} = \sum_{\alpha=0}^{2} W_\alpha^{\mathrm{e}} p_\alpha^{(k+1)} \tag{20}$$

with

$$\begin{aligned} p_0^{(k+1)} &= (p^{(k)})^2(2 - (p^{(k)})^2) \\ p_1^{(k+1)} &= p^{(k)}(1 + p^{(k)} - (p^{(k)})^2) \\ p_2^{(k+1)} &= p^{(k)}(2 - p^{(k)})\,. \end{aligned} \tag{21}$$

In an analogous way we can write the equations for $f^{(k)}$. Figure 6 shows one of the contributions to the renormalization of $f$. For the configuration $\alpha = 2$ we have two possible contributions depending on whether both or just one green subcell is hit by a lightning event. The first case occurs with probability $2f^{(k)}(1 - f^{(k)})$, the latter with probability $(f^{(k)})^2$. By summing these probabilities one obtains, for the configuration with $\alpha = 2$,

$$f_{\alpha=2}^{(k+1)} = f^{(k)}(2 - f^{(k)})\,. \tag{22}$$

We can write a renormalization equation for each configuration $\alpha$, and, averaging over all the configurations with their corresponding weights we obtain

$$f^{(k+1)} = \sum_{\alpha=2}^{4} W_\alpha^{\mathrm{g}} f_\alpha^{(k+1)} \tag{23}$$

with

$$\begin{aligned} f_2^{(k+1)} &= f^{(k)}(2 - f^{(k)}) \\ f_3^{(k+1)} &= f^{(k)}(3 - 3f^{(k)} + (f^{(k)})^2) \\ f_4^{(k+1)} &= f^{(k)}(4 - 6f^{(k)} + 4(f^{(k)})^2 - (f^{(k)})^3)\,. \end{aligned} \tag{24}$$

From equations (19) and (23) it is possible to write down the RG equation for $\theta^{(k+1)}$ as

$$\theta^{(k+1)} = \frac{f^{(k+1)}}{p^{(k+1)}} = \sum_{\alpha=2}^{\alpha=4} W_\alpha^{\mathrm{g}} f_\alpha^{(k+1)} \Big/ \sum_{\alpha=0}^{\alpha=2} W_\alpha^{\mathrm{e}} p_\alpha^{(k+1)}\,. \tag{25}$$

Inserting equations (21) and (24) in (25) one obtains the explicit expression of the RG equation for $\theta$:

$$\theta^{(k+1)} = \theta^{(k)} \frac{A + B\theta^{(k)} p^{(k)} + C(\theta^{(k)} p^{(k)})^2 + D(\theta^{(k)} p^{(k)})^3}{W_0^{\mathrm{e}} p^{(k)}(2 - (p^{(k)})^2) + W_1^{\mathrm{e}}(1 + p^{(k)} - (p^{(k)})^2) + W_2^{\mathrm{e}}(2 - p^{(k)})} \tag{26}$$

with $A = 2W_2^{\mathrm{g}} + 3W_3^{\mathrm{g}} + 4W_4^{\mathrm{g}}$, $B = -(W_2^{g} + 3W_3^{\mathrm{g}} + 6W_4^{\mathrm{g}})$, $C = W_3^{\mathrm{g}} + 4W_4^{\mathrm{g}}$ and $D = -W_4^{\mathrm{g}}$.

In order to close the RG equations we have to couple, as we did in the one-dimensional case, the dynamics to a stationarity condition that gives the renormalization equations for the density vector. We use the same stationarity condition (12) but with $d = 2$. This provides the renormalized density vector at scale $(k + 1)$, and couples the dynamical properties to the stationary ones.

By studying the flow diagram in the phase space of the parameters $(\boldsymbol{\rho}, p, \theta)$, we find that the RG equations show the fixed point $p^* = 0, \theta^* = 0$ and, following the same procedure used in the one-dimensional case, $\boldsymbol{\rho}^* = \left(\frac{2}{3}, \frac{1}{3}, 0\right)$.

As in the one-dimensional case, we reduce ourselves to the subset of the phase space $(p, \theta)$. In fact we can write the stationary densities as implicit functions of $p$ and $\theta$ and we have that a typical matrix element in the linearized RG transformation reads as

$$\frac{\mathrm{d}\theta^{(k+1)}}{\mathrm{d}\theta^{(k)}} = \frac{\partial\theta^{(k+1)}}{\partial\theta^{(k)}} + \frac{\partial\theta^{(k+1)}}{\partial\rho_1^{(k)}}\frac{\partial\rho_1^{(k)}}{\partial\theta^{(k)}} + \frac{\partial\theta^{(k+1)}}{\partial\rho_0^{(k)}}\frac{\partial\rho_0^{(k)}}{\partial\theta^{(k)}}\,. \tag{27}$$

It is worth noting that in the proximity of the fixed point $(p^*, \theta^*, \boldsymbol{\rho}^*)$ the derivatives $\partial\theta^{(k+1)}/\partial\rho_1^{(k)}$, $\partial\theta^{(k+1)}/\partial\rho_0^{(k)}$ are equal to zero. This means that at the fixed point the renormalization of the dynamical parameters is decoupled from the stationary properties of the system. After a little algebra we obtain that

$$\begin{aligned}
&\left.\frac{\mathrm{d}\theta^{(k+1)}}{\mathrm{d}\theta^{(k)}}\right|_{\theta^*,p^*,\boldsymbol{\rho}^*} = \left.\frac{2W_2^{\mathrm{g}} + 3W_3^{\mathrm{g}} + 4W_4^{\mathrm{g}}}{W_1^{\mathrm{e}} + 2W_2^{\mathrm{e}}}\right|_{\boldsymbol{\rho}^*} \simeq 2.6 \\
&\left.\frac{\mathrm{d}p^{(k+1)}}{\mathrm{d}p^{(k)}}\right|_{\theta^*,p^*,\boldsymbol{\rho}^*} = W_1^{\mathrm{e}} + 2W_2^{\mathrm{e}} l|_{\boldsymbol{\rho}^*} \simeq 1.0 \\
&\left.\frac{\mathrm{d}p^{(k+1)}}{\mathrm{d}\theta^{(k)}}\right|_{\theta^*,p^*,\boldsymbol{\rho}^*} = 0 \\
&\left.\frac{\mathrm{d}\theta^{(k+1)}}{\mathrm{d}p^{(k)}}\right|_{\theta^*,p^*,\boldsymbol{\rho}^*} = 0
\end{aligned} \tag{28}$$

the linearized RG equations being

$$\begin{pmatrix} p^{(k+1)} \\ \theta^{(k+1)} \end{pmatrix} = \begin{pmatrix} 1.0 & 0 \\ 0 & 2.6 \end{pmatrix} \begin{pmatrix} p^{(k)} \\ \theta^{(k)} \end{pmatrix}. \tag{29}$$

As in the one-dimensional case, there is just one relevant scaling field that corresponds to the eigenvalue larger than 1, $\lambda_2 = 2.6$. Therefore, also in this case we can identify a relevant parameter, $\theta$, which allows criticality just for its critical value $\theta^* = 0$, and which defines a repulsive direction in the phase space.

For the exponent $\nu$, which describes the divergence of the correlation length, or what is the same, the clusters' characteristic length $R \sim \theta^{-\nu}$, we have:

$$\nu = \frac{\log 2}{\log \lambda_2} = 0.73 \tag{30}$$

to be compared with the value $\nu = 0.58$ measured in [11, 12]. Also in this case we have a situation analogous to ordinary critical phenomena and the system shows an upper

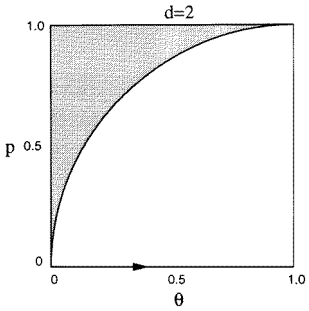


**Figure 7.** Phase space of the RG approach to the two-dimensional forest-fire model. The shadowed part is not described by our RG approach.

characteristic length in the cluster distribution for each finite value of $\theta$, i.e. criticality is just for $\theta = 0$.

The dynamical critical exponent $z$ can be calculated along the lines shown for the one-dimensional case. In this case we can also define the time scaling factor $\langle t \rangle = 2^z$ that links the time scale of burning processes at two consecutive levels of coarse graining ($T_{k+1}/T_k$). Note that $\langle t \rangle$ is the average number of subprocesses at scale $(k)$ necessary for the fire to fulfil the spanning condition for a cell at scale $(k+1)$. In this case the calculation is more complicated because the number of burning processes needed to have a fire on the scale $(k+1)$ depends upon the starting configurations at the smaller scale. By using the configuration of our RG scheme the above average can be written as

$$\langle t \rangle = \sum_{\alpha=2}^{4} W_\alpha^{\mathrm{g}} t_\alpha \tag{31}$$

having considered that $t_\alpha$ is the number of non-contemporary processes needed to burn a green configuration $\alpha$. It is easy to calculate $t_\alpha$ for each green configuration of figure 4, and by inserting the fixed-point parameters in the above equation we obtain the following result:

$$z = \frac{\log\langle t \rangle}{\log 2} = 1.11\,. \tag{32}$$

This value has to be compared with $z \simeq 1.04$ obtained in [20]. From the knowledge of $\nu$ and $z$ we can derive the exponent $\nu' = 0.81$ which gives the range of validity of our approach. In two dimensions it is very interesting to note that very close to the fixed point the double scale separation needed in the system is self-consistently verified in our approach in almost the white phase space (p–$\theta$). In fact, in the limit $\theta \to 0$, $p \to 0$ only the line $\theta = 0$ is not characterized correctly from our approach (see figure 7). This corresponds to the deterministic forest fire model with $f = 0$.

The other independent exponent $\tau$ describing the distribution of fire spreading can be obtained as follows. In this case the fire is represented by the clusters of connected sites interested by a burning process. As in [14] we define $K$ as the probability that an active relaxation process (i.e. fire) is limited between the scales $b^{(k)}$ and $b^{(k+1)}$ and it does not extend further:

$$K = \int_{b^{(k)}}^{b^{(k+1)}} P(r)\,\mathrm{d}r \Big/ \int_{b^{(k)}}^{\infty} P(r)\,\mathrm{d}r \tag{33}$$

where $P(r)\,\mathrm{d}r$ is the probability of having a burning cluster with radius between $r$ and $r+\mathrm{d}r$. In two dimensions with simple scaling arguments we can conclude that if $P(s) \sim s^{-\tau}$ and

$s \sim r^D$, then $P(r) \sim r^{-D(\tau-1)-1}$. Inserting this expression in (33) we obtain (in $d = 2$):

$$\tau = 1 - \frac{\log(1-K)}{D \log 2} . \tag{34}$$

We can thus use the scaling relation $\nu D = 1/(2-\tau)$ [20] to obtain a self-consistent relation for the exponent $\tau$. By inserting this scaling relation in the above equation for $\tau$ we obtain

$$\tau = \frac{1 - 2\nu S(K)}{1 - \nu S(K)} \tag{35}$$

where $S(K) = \log(1-K)/\log 2$. In our case $K$ is the probability that at a generic scale $(k)$ all the nearest neighbours of a burning tree are empty and then

$$K = (1 - \rho_1^{(k)})^4 . \tag{36}$$

In the scale-invariant regime ($\rho_1^{(k)} = \rho_1^*$), $K = 0.1975$ and then, by using the value $\nu = 0.73$ we obtain

$$\tau = 1.19 \tag{37}$$

$$D = 1.70 . \tag{38}$$

The exponent $\tau$ is in very good agreement with very accurate simulations [11, 12]. We will see in section 6 that it is possible to use a different strategy to calculate these last two exponents. In fact, from the knowledge of the fixed-point dynamics it is possible to calculate independently the fractal dimension of clusters (via the FST method), and by using the value obtained as an input in (35) we can evaluate the exponent $\tau$. This strategy gives a noticeable improvement in the results.

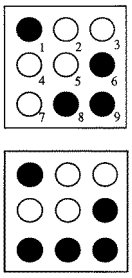


Empty site $\alpha = 4$



Green tree $\alpha = 5$

**Figure 8.** Two possible configurations of sites at the scale $b^{(k)}$ corresponding to an empty and a green cell, respectively, at the scale $b^{(k+1)}$ in $d = 2$ and for the $3 \times 3$ cell scheme. The numbers $1, \ldots, 9$ show the convention that denotes the different sites of the $3 \times 3$ cell.

**Table 1.** In this table we summarize our results for the critical exponents obtained with the different approximation schemes, compared with exact or experimental results.

| | $\nu$ | $z$ | $\tau$ | $\nu'$ | $D$ |
|---|---|---|---|---|---|
| $d = 1$ | | | | | |
| RG | 1.0 | 1.0 | 1.0 | 1.0 | 1.0 |
| Exact results[a] | 1.0 | 1.0 | 1.0 | 1.0 | 1.0 |
| $d = 2$ | | | | | |
| RG $2 \times 2$ | 0.73 | 1.11 | 1.19 | 0.81 | 1.7 |
| RG $3 \times 3$ | 0.65 | 1.02 | 1.17 | 0.66 | 1.9 |
| RG + FST $3 \times 3$ | 0.65 | 1.02 | 1.16 | 0.66 | 2.0 |
| Numerical results[b] | 0.58 | 1.04 | 1.15 | 0.6 | 1.95 |

[a] Exact results from [19].
[b] Numerical results from [11, 12].

We summarize our results for the one- and two-dimensional cases in table 1. In the table the values of the critical exponents calculated with our RG scheme are compared with the best estimates from numerical simulations of the FFM model and it can be noted that the agreement is very good. Nevertheless, it is worth noting that our results involve approximations usually present in real space renormalization methods: spanning condition, proliferation, etc. Therefore, it is possible to consider more complicated calculation schemes in order to improve the numerical values.

The simple calculation we have shown does not take into account all the connectivity properties which are at the heart of the forest-fire model. We can therefore improve the results systematically by considering cells of increasing size. We used a $3 \times 3$ cell-to-site renormalization in which a cell composed of nine sites at a generic scale $(k)$ is renormalized to a single site at scale $(k+1)$. The rules that define the spanning condition and the renormalization transformation are the same as given for the $2 \times 2$ case. Figure 8 shows an example of different cells with the corresponding coarse-grained site. The renormalization equations can be formally written as

$$p^{(k+1)} = \sum_{\alpha=0}^{\alpha=6} W_\alpha^{\mathrm{e}} p_\alpha^{(k+1)} \tag{39}$$

$$f^{(k+1)} = \sum_{\alpha=3}^{\alpha=9} W_\alpha^{\mathrm{g}} f_\alpha^{(k+1)} \tag{40}$$

where $W_\alpha^{\mathrm{e}}$, $W_\alpha^{\mathrm{g}}$ are the relative weights of the empty and green configurations, respectively. The functions $p_\alpha^{(k+1)}$ and $f_\alpha^{(k+1)}$ are derived by looking at the contribution of each starting configuration to the renormalization equations. The explicit evaluation of the above equations is very long and the calculation is shown in appendix B.

Once the explicit form of the RG equations is obtained we can study the flow diagram in the phase space along the same lines as the $2 \times 2$ scheme. It turns out that in this case also the RG transformation shows the fixed point $p^* = 0$, $\theta^* = 0$. We still find just one relevant scaling field whose corresponding eigenvalue is $\lambda_2 = 5.38$, and we therefore conclude that $\theta$ is a relevant control parameter which allows criticality just for its critical value $\theta = 0$. The exponent $\nu$ governing the divergence of the correlation length is

$$\nu = \frac{\log 3}{\log \lambda_2} = 0.65 \tag{41}$$

showing that the numerical result converges to the correct value with a refined renormalization scheme. The calculation of the dynamic critical exponent $z$ is rather laborious because it requires knowledge of all the possible fire spreading processes for each starting green cell. The detailed calculation is worked out in appendix B and we just report the final result

$$z = 1.02\,. \tag{42}$$

This result is in very good agreement with the numerical result $z = 1.04$, and suggests that the exact value is converging to $z = 1.0$. It is straightforward to calculate the other critical exponents by using the equations obtained previously:

$$\nu' = 0.66 \qquad \tau = 1.17 \qquad D = 1.9\,. \tag{43}$$

The results for the whole set of critical exponents are summarized in table 1. As can be seen, there is a consistent improvement in the numerical values obtained for the critical exponents. Moreover, it is important to note that the present general discussion about the

critical nature of the FFM is not affected by the approximations involved in our scheme. The existence of a relevant scaling field and the general structure of the flow diagram is, in fact, stable with different approximation schemes, even though a more refined calculation leads systematically to an improvement of the numerical values obtained for the critical exponents.

## 6. Alternative renormalization schemes

Real space renormalization groups are, in general, affected by the coarse-graining prescriptions. For instance, one can choose different spanning conditions, majority rules, lattice topologies, etc.

In order to prove that our renormalization scheme is consistent and gives reliable and stable results, we implemented different calculation schemes. In the previous sections we have been concerned with a cell-to-site renormalization transformation with the left–right spanning condition. The simplest generalization is to consider a double-spanning condition, i.e. the cell has to be spanned from left to right *and* from top to bottom. Another possible choice is a left-to-right *or* top-to-bottom spanning condition. Both these approximations and the one shown in the previous sections have to yield the same results for large cell calculations. We observed, in fact, that, repeating the $2 \times 2$ and the $3 \times 3$ calculations with the above spanning prescriptions, the numerical results converge to the values given by computer simulations. More importantly, the general features of the flow diagram in the phase space are robust with respect to the different approximations.

The FFM has so far been thought of as a site model. Of course it can be easily generalized to a bond version. In fact, the model can be defined in the same way as in the site case but with state variables associated to the bonds of a lattice. We therefore have that each bond can be empty, green or burning, and the dynamical rules governing the evolution of the system are the usual ones. The value of the critical exponents should be the same as for the site version of the model, as requested by universality.

Unfortunately, to our knowledge, there are no numerical simulations on bond FFM. Nevertheless, a renormalization-group treatment can be formulated along lines similar to those used for the site case.

We used a cell-to-bond transformation on the square lattice, in which each cell at scale $b$ is formed by five bonds at scale $b/2$ (see figure 9).

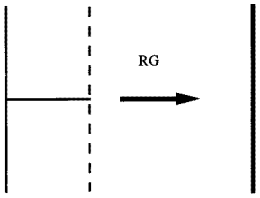


**Figure 9.** Scheme of the cell-to-bond transformation on a square lattice.

In this situation the spanning condition is a very natural one: the cell must be spanned from top to bottom and no other definitions are allowed. The bond topology, in fact, is the best one to take into account the connectivity properties of the model. In this case the results are in good agreement with numerical simulations and even for the $2 \times 2$ case we obtain results with a precision comparable with the results of the $3 \times 3$ cell-to-site calculation (for instance $\nu = 0.63$).

## 7. The fractal dimension of the fire clusters

In this section we want to show a different strategy of calculation of the cluster fractal dimension. Instead of using the scaling relation of section 5, we determine the fractal dimension independently, and we use the obtained value as an input for the calculation of $\tau$.

In order to calculate the exponent $D$ independently we use the fixed-scale transformation (FST) approach. This method focuses on the dynamics at a given scale and on accurately computing the correlations. The use of scale-invariant growth rules allows the generalization of these correlations to coarse-grained cells of any size and then to obtain the fractal dimension. The starting point of the FST method is the identification of the elementary configurations of the nearest-neighbour pair correlation (for details see [13]). In this respect it is convenient to consider correlations on a line perpendicular to the local growth direction. In two dimensions there are two types of different configuration: type 1 occurring with probability $C_1$, consisting of an occupied site (black) and an empty one (white), and type 2, occurring with probability $C_2$, with both sites occupied. The probability distribution $(C_1, C_2)$ can be simply related to the fractal dimension $D$ of the structure by [13]

$$D = 1 + \frac{\log(C_1^* + 2C_2^*)}{\log 2} \tag{44}$$

with $(C_1^*, C_2^*)$ representing the fixed point of the iterative transformation that links the probability distribution $(C_1, C_2)$ of a given intersection with the distribution of another intersection at the same scale but translated in the growth direction. The fixed point reflects the translational invariance of the structure. The matrix elements $M_{i,j}$ of the transformation represent the conditional probability that a given configuration $i$ will be followed, in the growth direction, by a configuration $j$. The fractal dimension can also be written in the form

$$D = 1 + \frac{\log \dfrac{2M_{1,2} + M_{2,1}}{M_{1,2} + M_{2,1}}}{\log 2}\,. \tag{45}$$

In this perspective FST is able to distinguish between fractal and non-fractal structures. In fact, if the matrix element $M_{1,1} = 0$ (and consequently $M_{2,1} = 0$) the corresponding structure is compact, i.e. the fractal dimension is equal to 2. In fact, in this case, the growth process does not produce holes at any scale. In the case of the forest-fire model we are going to analyse the $M_{1,1}$ matrix element in order to determine whether the fire clusters are compact or not. In order to do that we have to interpret the birth of a fire cluster as a growth process.

As we have already stressed, the critical point is characterized by a double separation of time scales. This means that each fire triggered by individual lightning does not overlap with other fires, thus clusters destroyed by fire are well defined objects. Therefore, the time scale separation regime assures that no lightning will strike during the growth of the cluster. When a site of the fire cluster is struck by lightning the entire clusters will burn in a very short time (compared to $1/p$). Looking at figure 10($a$), we consider the conditional probability $M_{1,1}$ that a configuration of type 1 is followed by another configuration of type 1. We consider open boundary conditions outside the growth column and we indicate with a white square a site not yet explored by the growth process. A white circle indicates an empty site. To first order the contribution to $M_{1,1}$ will be given by the probability that site 2 is empty, conditional on the fact that the growth process has to take place. Indicating

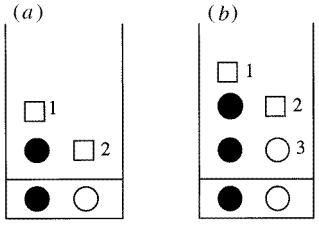


**Figure 10.** Scheme for the first- (*a*) and the second-order (*b*) contributions to the matrix element $M_{1,1}$ in the FST approach.

with $\Gamma = \rho_1 + p\rho_0$ the probability that a site is occupied at a certain time, one has

$$M^{\mathrm{I}}_{1,1} = \frac{\Gamma(1-\Gamma)}{2\Gamma(1-\Gamma)+\Gamma^2}\,. \tag{46}$$

where the denominator indicates the probability that the growth process takes place. At second order $M^{\mathrm{II}}_{1,1}$ will be given by the probability that site 3, which after the first step is empty, does not grow, conditional on the fact that the growth process takes place (see figure 10(*b*)). So we have

$$M^{\mathrm{II}}_{1,1} = \frac{(1-p)(2\Gamma(1-\Gamma)+\Gamma^2)}{p+(1-p)(2\Gamma(1-\Gamma)+\Gamma^2)} M^{\mathrm{I}}_{1,1} \tag{47}$$

which can be written in the short form

$$M^{\mathrm{II}}_{1,1} = M^{\mathrm{I}}_{1,1}(1-p)\frac{1}{1+p((1-A_2)/A_2)} \tag{48}$$

where $A_2 = 2\Gamma(1-\Gamma)+\Gamma^2$ with $A_2 < 1$. Iterating this procedure one can easily find

$$M^{N}_{1,1} = M^{\mathrm{I}}_{1,1}\prod_{n=2}^{N}(1-p)\frac{1}{1+p((1-A_n)/A_n)} \tag{49}$$

where the $A_n$ are the terms appearing at each order in the expression corresponding to (48). We then have

$$M^{N}_{1,1} < M^{\mathrm{I}}_{1,1}(1-p)^{N-1} \tag{50}$$

and in the limit $N \to \infty$ one obtains

$$\lim_{N\to\infty} M^{N}_{1,1} = 0 \tag{51}$$

for every small but finite value of $p$. We have, in fact, to perform the limit $N \to \infty$ and then the limit $p \to 0$. The fractal dimension of the fire clusters then tends, in the limit $N \to \infty$, to 2 (see equation (45)). The convergence as a function of the order of the process considered is slow, i.e. logarithmic, and we get $D = 2$ just at infinite order.

We can use this result in the calculation of the exponent $\tau$. By substituting $D = 2$ in equation (35) we obtain

$$\tau = 1 - \frac{\log(1-K)}{2\log 2} \tag{52}$$

and using the fixed-point value for $K$ we finally have

$$\tau = 1.16\,. \tag{53}$$

This value is in excellent agreement with numerical simulations, showing that the independent calculation of the fractal dimension leads to a noticeable improvement in the result.

## 8. Conclusions

In this paper we have shown a renormalization approach to the study of the critical state of forest-fire models. This approach represents an application of the dynamically driven renormalization group [16] and it follows the strategy used in [14] for sandpile models. The method is based on the following steps: first, we define the proper phase space with parameters that characterize the dynamical and stationary properties of the model. In this space, by coupling the renormalization of the dynamics to a stationary condition, i.e. the driving, we obtain the RG transformations, characterizing the evolution of the system under a scale change. By studying the flow diagram in the phase space we stress the presence of a repulsive fixed point for the RG equations, which corresponds to the existence of the relevant critical parameter $\theta$.

This means that the FFM is critical just along the line $\theta = 0$ of the phase space, $\theta$ being equivalent to the reduced temperature in the thermal phase transition. In other words $\theta$ is the control parameter of the model, and the critical state is reached only by a fine tuning of $\theta$ to its critical value.

In contrast to sandpile models, in fact, it is impossible to consider the FFM exactly at the critical point, i.e. in a subspace without relevant parameters. However, in both cases one can say that the critical state is reached just in the condition of a time scale separation. In the case of sandpile models this condition is hidden in the definition of the models but one can figure out a wider phase space with a relevant critical parameter, e.g. the driving parameter.

With the present approach it is therefore possible to clarify the role of the critical parameters $\theta$ and $p$ and the nature of the critical state. In addition, we are able to compute analytically the critical exponents characterizing the model in $d = 1$ and $d = 2$. Finally, it is important to note that the above general discussion is not affected by the approximations involved in the calculation scheme. Thus, we can introduce a naturally more refined RG scheme (larger cells, spanning condition, etc) in order to improve the values obtained for the critical exponents.

## Acknowledgments

Part of the work described here was carried out in collaboration with L Pietronero, and we are very grateful to him. We are also deeply indebted to B Drossel for very interesting discussions. It is a pleasure to thank P Bak, R Cafiero and P Grassberger for their suggestions.

## Appendix A

The weights of the configurations of empty or green subcells at scale $(k)$ corresponding, respectively, to empty or green cells at scale $(k+1)$ in $d = 2$ (figure 4) are given by

$$\begin{aligned} W_0^{\mathrm{e}} &= \Omega^{\mathrm{e}}\rho_0^4 \\ W_1^{\mathrm{e}} &= \Omega^{\mathrm{e}}4\rho_0^3\rho_1 \\ W_2^{\mathrm{e}} &= \Omega^{\mathrm{e}}4\rho_0^2\rho_1^2 \end{aligned} \tag{A1}$$

with

$$(\Omega^{\mathrm{e}})^{-1} = \rho_0^2(\rho_0^2 + 4\rho_1^2 + 4\rho_0\rho_1) \tag{A2}$$

and

$$W_2^{\mathrm{g}} = \Omega^{\mathrm{g}} 2\rho_0^2\rho_1^2$$
$$W_3^{\mathrm{g}} = \Omega^{\mathrm{g}} 4\rho_0\rho_1^3 \tag{A3}$$
$$W_4^{\mathrm{g}} = \Omega^{\mathrm{g}} \rho_1^4$$

with

$$(\Omega^{\mathrm{g}})^{-1} = \rho_1^2(\rho_1^2 + 2\rho_0^2 + 4\rho_0\rho_1)\,. \tag{A4}$$

The normalization conditions are obtained by requiring that the sum of the weights for configurations corresponding to an empty cell at scale $(k+1)$ (and analogously to a green cell) is 1. This condition is necessary in that, when we write down the renormalization equations, i.e. for $p^{(k)}$, we are looking for the conditional probability that, given an empty configuration at scale $(k+1)$, it becomes a green configuration at the same scale.

## Appendix B

In this section we show in detail a cell-to-site renormalization scheme in which a cell of $3 \times 3$ sites at a generic scale $(k)$ is renormalized in a single site at the scale $(k+1)$.

A cell at scale $(k+1)$ is considered *green* if a fire can pass through the entire cell spanning it in the horizontal direction. If the spanning condition is not satisfied the cell is *empty*. Finally, a green cell that contains at least one burning subcell is considered *burning*. Figure 8 shows an example of three kinds of site. We indicate with $\alpha$ the number of the green cells at the scale $(k)$ which compose a cell at the scale $(k+1)$. In table B1 we report, as a function of the parameter $\alpha$, the total number of cells $N_\alpha$ at the scale $(k+1)$ composed by $\alpha$ green subcells at the scale $(k)$, the number $N_\alpha^{\mathrm{g}}$ of green cells and the number $N_\alpha^{\mathrm{e}}$ of empty ones. The relative weight of each configuration is given by the probability of having the corresponding number of green and empty subcells

$$W_\alpha^{\mathrm{g}}(\boldsymbol{\rho}) = \rho^\alpha(1-\rho)^{9-\alpha}/\Omega_g$$
$$W_\alpha^{\mathrm{e}}(\boldsymbol{\rho}) = \rho^\alpha(1-\rho)^{9-\alpha}/\Omega_e \tag{B1}$$

**Table B1.** Number of configurations $N(\alpha)$ of kind $\alpha$ versus $\alpha$ in the $3 \times 3$ cell renormalization scheme, the number $N_\alpha^{\mathrm{g}}$ of green cells and the number $N_\alpha^{\mathrm{e}}$ of empty ones.

| $\alpha$ | $N(\alpha)$ | $N^{\mathrm{g}}(\alpha)$ | $N^{\mathrm{e}}(\alpha)$ |
|---|---|---|---|
| 0 | 1 | 0 | 1 |
| 1 | 9 | 0 | 9 |
| 2 | 36 | 0 | 36 |
| 3 | 84 | 3 | 81 |
| 4 | 126 | 22 | 104 |
| 5 | 126 | 59 | 67 |
| 6 | 84 | 67 | 17 |
| 7 | 36 | 36 | 0 |
| 8 | 9 | 9 | 0 |
| 9 | 1 | 1 | 0 |

with the normalization factors:

$$\begin{aligned}\Omega_g &= 1/3^9\left[\sum_\alpha 2^\alpha N_\alpha^{\mathrm{g}}\right]\\ \Omega_e &= 1/3^9\left[\sum_\alpha 2^{9-\alpha} N_\alpha^{\mathrm{e}}\right].\end{aligned} \tag{B2}$$

As in the $2 \times 2$ case we consider the site configurations in the stationary state uncorrelated. The rules to define the renormalization transformation are the same given for the previous cases. The renormalization equation for the parameter $p$ can be formally written in the form (39) that we rewrite here for the sake of clarity:

$$p^{(k+1)} = \sum_{\alpha=0}^{6} W_\alpha^{\mathrm{e}} p_\alpha^{(k+1)} \tag{B3}$$

with

$$p_\alpha^{(k+1)} = \sum_{i=1}^{N_\alpha^{\mathrm{e}}} \Pi_i^\alpha(p^{(k)})\,. \tag{B4}$$

Analogously one can write the corresponding equations (40) for $f$ as

$$f^{(k+1)} = \sum_{\alpha=3}^{9} W_\alpha^{\mathrm{g}} f_\alpha^{(k+1)} \tag{B5}$$

with

$$f_\alpha^{(k+1)} = \sum_{j=1}^{N_\alpha^{\mathrm{g}}} \Phi_j^\alpha(f^{(k)})\,. \tag{B6}$$

We introduce the functions $\Pi_i^\alpha$ and $\Phi_j^\alpha$ which represent the unknown parts of the renormalization equations; they are derived considering the contribution of each single configuration (green or empty) to the renormalization equations. The whole operation is long and tedious.

For sake of simplicity we will report just the expressions of the contributions linear in $p^{(k)}$ and in $f^{(k)}$. These terms are the only ones that contribute to the matrix elements of the transformation linearized around the fixed point, and, thus, the only ones that contribute to the calculation of the critical exponents describing the approach to the critical point. In fact it turns out that the renormalization equations present, also in this case, the fixed point

$$p^* = 0 \qquad \theta^* = 0\,. \tag{B7}$$

We can then cast equations (B4) and (B6) in the form

$$\begin{aligned}p_\alpha^{(k+1)} &= p^{(k)} \sum_i n_i^\alpha + \mathrm{O}({p^{(k)}}^2) \qquad i = 1, N_\alpha^{\mathrm{e}}\\ f_\alpha^{(k+1)} &= f^{(k)} \sum_j m_j^\alpha + \mathrm{O}({f^{(k)}}^2) \qquad j = 1, N_\alpha^{\mathrm{g}}\end{aligned} \tag{B8}$$

and equations (B4) and (B6) in the form

$$\begin{aligned}p^{(k+1)} &= p^{(k)}\left[\sum_\alpha W_\alpha^{\mathrm{e}} \sum_i^{N_\alpha^{\mathrm{e}}} n_i^\alpha\right] + \mathrm{O}({p^{(k)}}^2)\\ f^{(k+1)} &= f^{(k)}\left[\sum_\alpha W_\alpha^{\mathrm{g}} \sum_j^{N_\alpha^{\mathrm{g}}} m_j^\alpha\right] + \mathrm{O}({f^{(k)}}^2)\,.\end{aligned} \tag{B9}$$

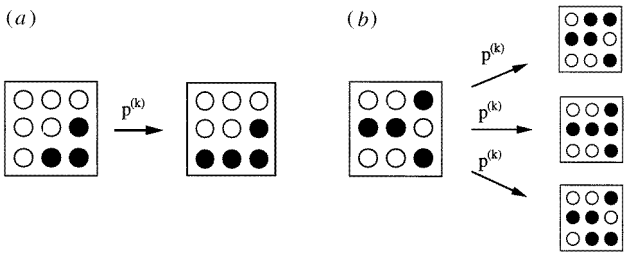


**Figure B1.** Two examples of contributions to the renormalization of $p$ in the $3 \times 3$ cell scheme.

In the previous equations $n_i^\alpha$ and $m_j^\alpha$, indicate, respectively, the coefficients, which take integer values, of the first-order contribution to the renormalization of $p$ and $f$. For the sake of clarity we show in figure B1 two examples of the contributions to the renormalization of $p$. In figure B1($a$) the contribution to $n_i^\alpha$ with $\alpha = 3$ is one in that there is just one possibility that can lead to the growth at scale $(k+1)$ in the starting configuration by the growth of just one tree at scale $(k)$. In figure B1($b$) there are three different processes that contribute to the growth of the starting configuration at scale $(k+1)$ and the corresponding $n_i^\alpha$ is three.

Starting from (B9) it is possible to write the renormalization equation for $\theta$:

$$\theta^{(k+1)} = \frac{f^{(k+1)}}{p^{(k+1)}} = \theta^{(k)} \frac{\left[\sum_\alpha W_\alpha^{\mathrm{g}} \sum_j^{N_\alpha^{\mathrm{g}}} m_j^\alpha\right] + f^{(k)}[\cdots]}{\left[\sum_\alpha W_\alpha^{\mathrm{e}} \sum_i^{N_\alpha^{\mathrm{e}}} n_i^\alpha\right] + p^{(k)}[\cdots]} \tag{B10}$$

where the $[\cdots]$ indicate the higher-order contributions to the renormalization of $p$ and $f$.

As in the $2 \times 2$ scheme we close the renormalization equations by coupling to them the stationarity condition (12) which provides the renormalized density vector at scale $(k+1)$ and it couples the dynamical properties to the stationary ones. The fixed point, as in the $2 \times 2$ scheme, is given by $\boldsymbol{\rho}^* = \left(\frac{2}{3}, \frac{1}{3}, 0\right)$.

Let us pass to the calculation of the critical exponents in this new scheme. Along the same lines as the $2 \times 2$ scheme, we get

$$\begin{aligned}
&\left.\frac{\mathrm{d}\theta^{(k+1)}}{\mathrm{d}\theta^{(k)}}\right|_{\theta^*,p^*,\boldsymbol{\rho}^*} = \left.\frac{\sum_\alpha W_\alpha^{\mathrm{g}} \sum_j^{N_\alpha^{\mathrm{g}}} m_j^\alpha}{\sum_\alpha W_\alpha^{\mathrm{e}} \sum_i^{N_\alpha^{\mathrm{e}}} n_i^\alpha}\right|_{\boldsymbol{\rho}^*} \simeq 5.38 \\
&\left.\frac{\mathrm{d}p^{(k+1)}}{\mathrm{d}p^{(k)}}\right|_{\theta^*,p^*,\boldsymbol{\rho}^*} = \left.\sum_\alpha W_\alpha^{\mathrm{e}} \sum_i^{N_\alpha^{\mathrm{e}}} n_i^\alpha\right|_{\boldsymbol{\rho}^*} \simeq 0.85 \\
&\left.\frac{\mathrm{d}p^{(k+1)}}{\mathrm{d}\theta^{(k)}}\right|_{\theta^*,p^*,\boldsymbol{\rho}^*} = 0 \\
&\left.\frac{\mathrm{d}\theta^{(k+1)}}{\mathrm{d}p^{(k)}}\right|_{\theta^*,p^*,\boldsymbol{\rho}^*} = 0\,.
\end{aligned} \tag{B11}$$

We still find just one relevant scaling field that corresponds to the eigenvalue greater than one, $\lambda_2 = 5.38$. Therefore, in this case also we can identify a relevant parameter, $\theta$, which allows criticality just for its critical value $\theta^* = 0$, and which defines a repulsive direction in the phase space.

By using the relevant eigenvalue we obtain that the characteristic length exponent is $\nu = 0.65$. This result shows that the enhanced method, which uses $3 \times 3$ cells, allows us to

improve the accuracy of our calculation (compare the result $\nu = 0.73$ obtained in the $2 \times 2$ scheme) and it gives an indication of the systematic nature of the approach.

The other independent critical exponent is the dynamical exponent $z$. Its calculation in the $3 \times 3$ scheme is rather laborious in that, for each configuration of type $\alpha$, we have to take into account all the possible processes by which the fire can span the green cell.

The $z$ exponent in this case is defined, in the asymptotic limit $k \to \infty$, by the ratio

$$\frac{T^{(k+1)}}{T^{(k)}} = 3^z \tag{B12}$$

where $T^{(k)}$ is the average time of a dynamical process (fire) at scale $(k)$. The time scale $T^{(k+1)}$ can be obtained as a function of the time scale $T^{(k)}$ from the RG equations. In fact the renormalized dynamical process is given by the weighted average series of subprocesses at scale $(k)$, whose time scale is given by $T^{(k)}$. We therefore have

$$T^{(k+1)} = \langle t \rangle T^{(k)} \tag{B13}$$

where $\langle t \rangle$ is the subprocesses at scale $(k)$ needed to have a relaxation process at scale $(k+1)$. In our scheme we have

$$\langle t \rangle = \sum_{\alpha} W_{\alpha}^{g} \sum_{h=1}^{N_{\alpha}^{g}} \langle \tau_h \rangle_{\alpha} \tag{B14}$$

where $\langle \tau_h \rangle_{\alpha}$ is the average number of subprocesses in which the $h$th configuration of type $\alpha$ burns down. In the calculation of the elements $\langle \tau_h \rangle_{\alpha}$ we have to take into account that a relaxation process (a fire) can start from any of the trees at scale $(k)$ which belongs to the connected cluster that allows the spanning rule to be satisfied. Figure B2 shows an example of the calculation of $\langle \tau_h \rangle_{\alpha}$ in a simple case.

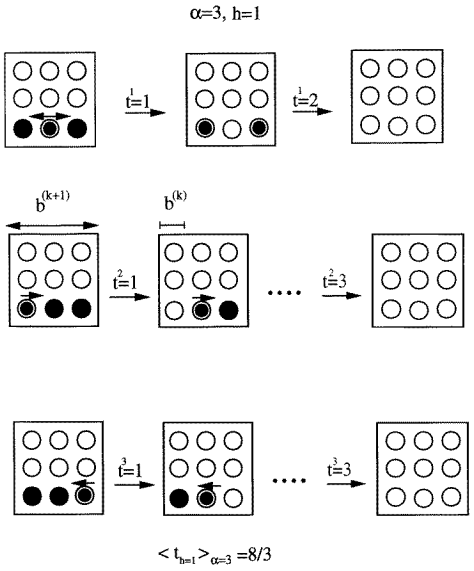


**Figure B2.** Example of the calculation of a contribution $\langle \tau_h \rangle_{\alpha}$ in the $3 \times 3$ cell scheme.

By comparing (B13) and (B14) we obtain $\langle t \rangle = 3^z$ and then

$$z = \frac{\log \sum_{\alpha} W_{\alpha}^{g} \sum_{h=1}^{N_{\alpha}^{g}} \langle \tau_h \rangle_{\alpha}}{\log 3} = 1.02\,. \tag{B15}$$

Other exponents can easily be evaluated along the lines shown for the $2 \times 2$ case, and the results are discussed in section 5.

## References


[1] Bak P, Chen K and Tang C 1990 *Phys. Lett.* **147A** 297
[2] Drossel B and Schwabl F 1992 *Phys. Rev. Lett.* **69** 1629
[3] Bak P, Tang C and Wiesenfeld K 1987 *Phys. Rev. Lett.* **59** 381; 1988 *Phys. Rev.* A **38** 364
[4] Witten T A and Sander L M 1981 *Phys. Rev. Lett* **47** 1400
[5] Niemeyer L, Pietronero L and Wiesmann H J 1984 *Phys. Rev. Lett.* **52** 1033
[6] Bak P and Sneppen K 1993 *Phys. Rev. Lett.* **71** 4083
[7] Wilkinson D and Willemsen J F 1983 *J. Phys. A: Math. Gen.* **16** 3365
[8] Bak P and Tang C 1989 *J. Geophys. Res.* B **94** 15635–7
Bak P, Chen K, Scheinkmen J and Woodford M 1993 *Ric. Economiche* **47** 3
[9] Grassberger P and Kantz H 1991 *J. Stat. Phys.* **63** 685
[10] Moßner W K, Drossel B and Schwabl F 1992 *Physica* A **190** 205
[11] Grassberger P 1993 *J. Phys. A: Math. Gen.* **26** 2081
[12] Henley C L 1993 *Phys. Rev. Lett.* **71** 2741
[13] Pietronero L, Erzan A and Evertsz C 1988 *Phys. Rev. Lett* **61** 861
Cafiero R, Pietronero L and Vespignani A 1993 *Phys. Rev. Lett.* **70** 3939
For a review see Erzan A, Pietronero L and Vespignani A 1995 *Rev. Mod. Phys.* **67** 545
[14] Pietronero L, Vespignani A and Zapperi S 1994 *Phys. Rev. Lett.* **72** 1690
Vespignani A, Zapperi S and Pietronero L 1995 *Phys. Rev.* E **51** 1711
[15] Ben Hur A, Hallgass R and Loreto V 1996 *Phys. Rev.* E, submitted
[16] Vespignani A, Zapperi S and Loreto V 1996 Dynamically driven renormalization group *J. Stat. Phys.* submitted
[17] Loreto V, Pietronero L, Vespignani A and Zapperi S 1995 *Phys. Rev. Lett.* **75** 465
[18] Christensen K, Flyvbjerg H and Olami Z 1993 *Phys. Rev. Lett.* **71** 2737
[19] Drossel B, Clar S and Schwabl F 1993 *Phys. Rev. Lett.* **71** 3739
[20] Clar S, Drossel D and Schwabl F 1994 *Phys. Rev.* E **50** 1009
[21] Drossel B and Schwabl F 1993 *Physica* A **204** 212